



Provided by the author(s) and University College Dublin Library in accordance with publisher policies. Please cite the published version when available.

<b>Title</b>	Generalized Least Squares Based Channel Estimation for High Data Rate FBMC-OQAM
<b>Authors(s)</b>	Singh, Vibhutesh Kumar; Flanagan, Mark F.; Cardiff, Barry
<b>Publication date</b>	2018-06-28
<b>Publication information</b>	2018 25th International Conference on Telecommunications, ICT 2018
<b>Conference details</b>	The 25th International Conference on Telecommunications (ICT 2018), Saint-Malo, France, 26-28 June 2018
<b>Publisher</b>	IEEE
<b>Link to online version</b>	<a href="https://u-bretagne-iloire.fr/ict-2018-25th-international-conference-telecommunication">https://u-bretagne-iloire.fr/ict-2018-25th-international-conference-telecommunication</a>
<b>Item record/more information</b>	<a href="http://hdl.handle.net/10197/11133">http://hdl.handle.net/10197/11133</a>
<b>Publisher's statement</b>	© 2018 IEEE. Personal use of this material is permitted. Permission from IEEE must be obtained for all other uses, in any current or future media, including reprinting/republishing this material for advertising or promotional purposes, creating new collective works, for resale or redistribution to servers or lists, or reuse of any copyrighted component of this work in other works.
<b>Publisher's version (DOI)</b>	10.1109/ICT.2018.8464892

Downloaded 2020-03-05T17:28:15Z

The UCD community has made this article openly available. Please share how this access benefits you. Your story matters! (@ucd\_oa)



Some rights reserved. For more information, please see the item record link above.



# Generalized Least Squares Based Channel Estimation for High Data Rate FBMC-OQAM

Vibhutesh Kumar Singh, Mark F. Flanagan and Barry Cardiff

School of Electrical and Electronic Engineering

University College Dublin, Belfield, Dublin 4, Ireland

Email: vibhutesh.k.singh@ieee.org, mark.flanagan@ieee.org, barry.cardiff@ucd.ie

**Abstract**—This paper addresses the problem of preamble-based Channel Estimation (CE) in filter bank multi-carrier systems with offset quadrature amplitude modulation (FBMC-OQAM), a task that is problematic due to the presence of intrinsic Inter-Carrier Interference (ICI) and Inter-Symbol Interference (ISI). In this work, we present a theoretical analysis of the Mean Squared Error (MSE) of several CE schemes based on the virtual symbol (VS) approach such as the Interference Cancellation Method (ICM) and the Interference Approximation Method (IAM). We also propose and analyze a generalized least squares (GLS) based CE scheme which is capable of achieving improved performance by taking into account the correlation properties of the noise and interference among sub-carriers. Simulation results are presented which verify the accuracy of the theoretical analysis, and also demonstrate that the proposed GLS-based estimation method yields an improvement of almost 3dB in the CE-MSE with respect to the VS-based approach. Finally it is shown that, for higher-order modulation schemes, this CE-MSE reduction translates into significant improvement in the system's overall bit error rate (BER) performance with only minor additional complexity.

## I. INTRODUCTION

FBMC-OQAM is a multi-carrier waveform which is being strongly considered as an alternative to cyclic-prefix based orthogonal frequency division multiplexing (CP-OFDM) for the upcoming 5G communication standard. The main advantages of FBMC-OQAM in this context are its increased spectral efficiency, extremely low out-of-band emissions (OOBE) and immunity to synchronization errors. It is thus a strong contender as a future 5G waveform [1].

Accurate and efficient channel estimation (CE) is an essential part of the successful operation of FBMC-OQAM. A substantial amount of recent research work has concentrated on the problem of preamble-based channel estimation in FBMC-OQAM [2], which is complicated due to the intrinsic imaginary interference (ICI/ISI) experienced by transmitted symbols. The most widely established CE techniques for FBMC-OQAM follow a virtual symbol based approach, namely the interference approximation method (IAM) [3] and the interference cancellation method (ICM) [4]. These methods are founded on the assumption of no interference from the data frame to the preamble sequence (in fact, only interference from the first-order symbol neighborhood is considered in the preamble). However, all of these schemes suffer from severe CE error floors at high SNR ( $> 20$  dB), which is due to the assumptions of zero data interference on the preamble, local invariance of

the channel in a small frequency-time (FT) neighborhood, and independence of interference-plus-noise contributions on different sub-carriers [5]. Thus, efficiently addressing the problem of channel estimation in the presence of data interference on the preamble, and taking into account the non-independence of interference-plus-noise contributions on different sub-carriers, is still an open problem.

This paper presents a theoretical analysis of the CE-MSE of conventional virtual symbol (VS) based FBMC-OQAM CE schemes and their GLS-based variants, by taking into account the interference from the data frame as well the correlation of noise and interference, aspects which have been generally ignored in existing works e.g., [5], [6]. It is shown that this MSE analysis provides performance predictions which are in very good agreement with results obtained through simulation. We also propose a novel channel estimation technique based on the application of generalized least squares (GLS) estimation [7], [8] which is capable of taking into account the statistical properties of the interference and noise. It is shown that GLS-based CE method has almost 3dB improvement in the CE-MSE floor with respect to conventional VS-based schemes, i.e., IAM-R, IAM-C [2] and ICM. We also show that for higher-order modulation, such lowering of the MSE floor can bring significant improvement in the system BER. Finally, it is shown that the performance analysis provides accurate performance predictions also in the presence of mobility.

**Notations:** Vectors and matrices are denoted by bold letters. For a matrix  $\mathbf{A}$ ,  $[\mathbf{A}]_{i,j}$  denotes its  $(i,j)$  entry. Superscripts  $T$  and  $\mathcal{H}$  denote transpose and conjugate transpose of matrices.  $\Re(x)$  denotes the real part of a complex number  $x$ , while  $x^*$  denotes its complex conjugate.  $\mathbb{Z}$  denotes the set of integers,  $\mathbb{E}$  denotes the expectation operator, and  $j = \sqrt{-1}$ .

## II. FBMC-OQAM SYSTEM MODEL

### A. FBMC-OQAM signal

The discrete-time baseband equivalent of an FBMC-OQAM signal having  $M$  sub-carriers is given by [9]

$$s(l) = \sum_{m=0}^{M-1} \sum_{n=-\infty}^{+\infty} a_{m,n} g_{m,n}(l) \quad \forall l \in \mathbb{Z}, \quad (1)$$

where the pair  $(m,n)$  indexes a frequency-time (FT) resource element. Centred on each FT point  $(m,n)$ , a real-valued PAM

symbol  $a_{m,n}$  modulates  $g_{m,n}(l)$ , which is a phase, frequency and time shifted version of a prototype impulse response  $g(l)$ , i.e., (assuming  $M$  to be even)

$$g_{m,n}(l) \triangleq g\left(l - \frac{nM}{2}\right) e^{j\frac{2\pi}{M}m(l - \frac{Lg-1}{2})} e^{j\varphi_{m,n}} \quad (2)$$

where  $g$  is a real linear-phase unit-energy impulse with length  $L_g = KM$ , where  $K$  is the time overlapping factor and  $\varphi_{m,n} \triangleq (m+n)\frac{\pi}{2} + mn\pi$ . Thus

$$s(l) = \sum_{m=0}^{M-1} \sum_{n=-\infty}^{+\infty} a_{m,n} j^{m+n} e^{j2\pi\frac{ml}{M}} g\left(l - \frac{nM}{2}\right) \beta_{m,n} \quad (3)$$

where  $\beta_{m,n} \triangleq e^{j2\pi m(\frac{n}{2} - \frac{KM-1}{2M})}$ .

A matched filter receiver attempting to detect symbol  $a_{p,q}$  has response  $g_{p,q}^*$  and its output will contain contributions from each transmitted symbol  $a_{m,n}$  given by  $a_{m,n}\xi_{m,n}^{p,q}$ , where

$$\xi_{m,n}^{p,q} \triangleq \sum_{l=-\infty}^{\infty} g_{m,n}(l) g_{p,q}^*(l). \quad (4)$$

It can be shown that these interference coefficients  $\xi_{m,n}^{p,q}$  have a frequency-symmetry property which can be expressed as

$$\xi_{p-\delta_p, q+\delta_q}^{p,q} = (-1)^{\delta_q} (\xi_{p+\delta_p, q-\delta_q}^{p,q})^*; \quad \forall p, q, \delta_p, \delta_q \in \mathbb{Z}. \quad (5)$$

As per [9], we use a prototype filter designed such that the following real orthogonality condition is satisfied:

$$\Re(\xi_{m,n}^{p,q}) = \Re\left(\sum_{l=-\infty}^{\infty} g_{m,n}(l) g_{p,q}^*(l)\right) = \delta_{m,p} \delta_{n,q} \quad (6)$$

where  $\delta_{r,s}$  denotes the Kronecker delta function. This condition causes the matched filter output to contain *purely imaginary intrinsic interference* as illustrated in Table I.

### B. Reception with time-dispersive channel

This paper is concerned with preamble-based channel estimation techniques, and thus the time-dispersive channel is assumed to be time-invariant for the duration of the preamble and the first data-bearing symbols. Additionally, under the mild assumption that the channel delay spread is small compared to the FMBC symbol duration, we can define a channel vector  $\mathbf{h} = [h_0 \ h_1 \ \dots \ h_{M-1}]$  whose  $i$ -th entry  $h_i$  is the channel gain in sub-carrier  $i$ , and is normalized such that  $\mathbb{E}[|h_i|^2] = 1$ . The output of the  $(p, q)^{th}$  matched filter is

$$\begin{aligned} y_{p,q} &= \sum_{m,n} \tilde{h}_m \xi_{m,n}^{p,q} a_{m,n} + w_{p,q} \\ &= h_p a_{p,q} + \sum_{(m,n) \neq (p,q)} \tilde{h}_m \xi_{m,n}^{p,q} a_{m,n} + w_{p,q} \end{aligned} \quad (7)$$

where the summation in (7) represents the *intrinsic interference* and  $w_{p,q} = \sum_l \eta(l) g_{p,q}^*(l)$  is colored noise affecting the FT point  $(p, q)$ , which is a filtered version of the complex AWGN  $\eta(l) \sim \mathcal{N}(0, \sigma^2)$ .  $w_{p,q}$  has variance  $E[|w_{p,q}|^2] = \sigma^2$  and is correlated among sub-carriers with covariance  $E[w_{p,q} w_{m,n}^*] = \sigma^2 \xi_{m,n}^{p,q}$ . If  $\tilde{\mathbf{h}} \approx \mathbf{h}$  is an estimate of the channel vector then, by

TABLE I  
NUMERICAL EXAMPLE OF  $\xi_{m,n}^{p,q}$ ,  $p$  EVEN, FOR THE PHYDYAS FILTER [10]. THE ENTRIES MARKED WITH  $\dagger$  ARE NEGATED FOR  $p$  ODD.

	q-3	q-2	q-1	n=q	q+1	q+2	q+3
p+2	0	0	0	0	0	0	0
p+1	-j0.0429 $\dagger$	-j0.125	-j0.2058 $\dagger$	-j0.2393	-j0.2058 $\dagger$	-j0.125	-j0.0429 $\dagger$
m=p	j0.0668 $\dagger$	0	j0.5644 $\dagger$	1	-j0.5644 $\dagger$	0	-j0.0668 $\dagger$
p-1	-j0.0429 $\dagger$	j0.125	-j0.2058 $\dagger$	j0.2393	-j0.2058 $\dagger$	j0.125	-j0.0429 $\dagger$
p-2	0	0	0	0	0	0	0

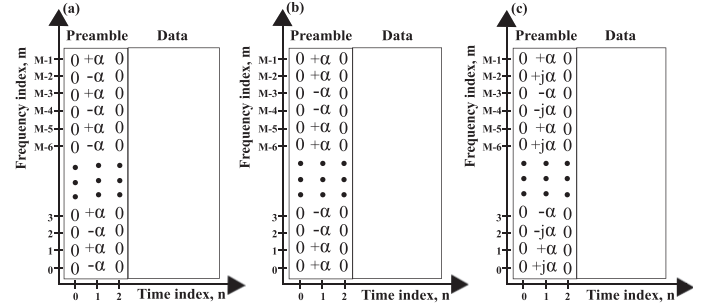


Fig. 1. Block preamble arrangement of (a) ICM; (b) IAM-R; and (c) IAM-C [2]. Here  $\alpha$  is any real-valued symbol.

ignoring the interference term, a one-tap zero-forcing equalizer can be used to estimate the data symbols via

$$\tilde{a}_{p,q} \triangleq \Re\left(\frac{y_{p,q}}{\tilde{h}_p}\right) \approx a_{p,q}. \quad (8)$$

This paper considers preamble-based approaches which are used to form the channel estimates  $\tilde{\mathbf{h}}$  required for the above equalizer.

## III. PREAMBLE-BASED CHANNEL ESTIMATION

### A. Virtual symbol approach

Fig. 1 shows the preamble symbol arrangements of IAM, IAM-R and IAM-C, where  $\alpha$  is a real-valued preamble symbol. For such a preamble structure, a simple method to estimate the channel is to assume that for each sub-carrier  $p$ , the sub-carrier gain  $h_p$  is constant over the immediate sub-carrier neighborhood and that the interference contribution from the data portion is insignificant. Accordingly

$$y_{p,q} \approx h_p \sum_{(m,n) \in \Theta_{p,q}} \xi_{m,n}^{p,q} a_{m,n} + w_{p,q} \triangleq h_p c_{p,q} + w_{p,q} \quad (9)$$

where  $\Theta_{p,q} \triangleq \{(m, n) : |p-m| \leq 1, |q-n| \leq 1\}$ . For simplicity we define  $y_p \triangleq y_{p,1}$  and  $c_p \triangleq c_{p,1}$ , leading to the channel estimate

$$\tilde{h}_p \triangleq \frac{y_p}{c_p} \approx h_p \quad (10)$$

Using (5) and Table I, formulae for  $c_p$  for each of the three schemes can be computed as per Table II.

TABLE II  
VIRTUAL SYMBOL AND MSE FOR VARIOUS PREAMBLE STRUCTURES

Scheme	$c_{p,q} \triangleq \sum_{(m,n) \in \Theta_{p,q}} \xi_{m,n}^{p,q} a_{m,n}$	$ c_p $	MSE floor (relative to ICM), from (17)
ICM	$c_p = a_{p,1}$	$ \alpha $	0dB
IAM-R	$c_p = a_{p,1} \left( 1 \pm 2\xi_{p+1,1}^{p,1} \right)$	$\approx 1.11 \alpha $	-0.9dB
IAM-C	$c_p = a_{p,1} \left( 1 \pm j2\xi_{p+1,1}^{p,1} \right)$	$\approx 1.48 \alpha $	-3.4dB

### B. Proposed Generalized Least Squares Based Estimation

We propose a new estimation algorithm for  $\tilde{h}_p$  that involves taking two frequency-consecutive received samples, i.e.,  $\mathbf{y}_p = [y_p \ y_{p+1}]^T$ , and expressing these as two weighted observations of  $h_p$  perturbed by additive correlated noise; this can be solved using a generalized least squares (GLS) approach. The received observation vector can be expressed as

$$\mathbf{y}_p = \mathbf{c}_p h_p + \mathbf{I}_p + \mathbf{w}_p \quad (11)$$

where  $\mathbf{c}_p \triangleq [c_p \ c_{p+1}]^T$  is a vector of virtual symbols as defined in Section III-A.  $\mathbf{I}_p$  and  $\mathbf{w}_p \triangleq [w_{p,1} \ w_{p+1,1}]^T$  are the vectors of interference and noise respectively affecting the observation vector  $\mathbf{y}_p$ . Note that  $\mathbf{I}_p$  contains contributions from random data symbols; these are assumed to have zero mean and variance  $\sigma_a^2$ . Furthermore, we note that the two elements of  $\mathbf{I}_p$  are correlated as they both depend on the same data symbols, and the two elements of  $\mathbf{w}_p$  also correlated; hence the need for GLS as opposed to the ordinary least squares (OLS) algorithm. Denote by  $|h_p|^2 \mathbf{\Omega}$  the covariance matrix of  $\mathbf{I}_p + \mathbf{w}_p$ . Then, assuming the use of the PHYDYAS prototype filter<sup>1</sup>, using Table I and the symmetry condition (5) we obtain

$$\begin{aligned} [\mathbf{\Omega}]_{1,1} &= \sigma_a^2 \{ |\xi_{p,4}^{p,1}|^2 + 2|\xi_{p+1,3}^{p,1}|^2 + 2|\xi_{p+1,4}^{p,1}|^2 + \eta^{-1} \} \\ [\mathbf{\Omega}]_{1,2} &= \sigma_a^2 \{ \xi_{p,4}^{p,1} \xi_{p,4}^{*p+1,1} + \xi_{p+1,4}^{p,1} \xi_{p+1,4}^{*p+1,1} + \xi_{p+1,1}^{p,1} \eta^{-1} \} \\ [\mathbf{\Omega}]_{2,2} &= [\mathbf{\Omega}]_{1,1} \text{ and } [\mathbf{\Omega}]_{2,1} = [\mathbf{\Omega}]_{1,2}^* \end{aligned}$$

where  $\eta \triangleq \frac{|h_p|^2 \sigma_a^2}{\sigma^2}$  is a measure of the receiver's instantaneous signal-to-noise ratio<sup>2</sup>. The GLS estimate is then given by

$$\tilde{h}_p = \mathbf{g}_p^T \mathbf{y}_p = (\mathbf{c}_p^H \mathbf{\Omega}^{-1} \mathbf{c}_p)^{-1} \mathbf{c}_p^H \mathbf{\Omega}^{-1} \mathbf{y}_p. \quad (12)$$

Note that  $\eta$  depends on  $h_p$ , meaning that  $\mathbf{\Omega}$  (and hence  $\mathbf{g}_p$ ) cannot be computed exactly without prior knowledge of  $h_p$ . For this reason, we replace  $\eta$  by  $\eta^3 \mathbb{E}[\eta] = \frac{\sigma_a^2}{\sigma^2}$  in the GLS estimator to obtain

$$\tilde{h}_p = \hat{\mathbf{g}}_p^T \mathbf{y}_p \quad \text{where} \quad \hat{\mathbf{g}}_p \triangleq \mathbf{g}_p \Big|_{\eta = \frac{\sigma_a^2}{\sigma^2}} \quad (13)$$

Note that  $\tilde{h}_p$  is simply a fixed linear combination of the two elements of  $\mathbf{y}_p$  and is thus easily implemented. Also note

<sup>1</sup>The covariance matrix can be easily derived in a similar manner for any other prototype filter.

<sup>2</sup>It can easily be shown that  $\mathbf{\Omega}$  depends only on the parity of  $p$ ; thus, only the details regarding two different matrices  $\mathbf{\Omega}$  need be stored at the receiver (for  $p = 0$  and for  $p = 1$ ).

<sup>3</sup>Note that at high SNR, the effect of this replacement becomes negligible, as the term  $\eta^{-1}$  tends to zero.

that the proposed channel estimation technique can easily be extended to the case of more than two adjacent sub-carriers, although the use of such an extension is restricted to channels having low frequency selectivity.

### IV. MSE ANALYSIS OF CHANNEL ESTIMATION TECHNIQUES

All of the channel estimation schemes presented above have in common two principal assumptions: a) the channel is locally constant<sup>4</sup>; and b) distant symbols contribute negligible interference. The second of these assumptions is weak and leads to a floor in the channel estimation MSE. In this section, we theoretically analyze the normalized mean squared error (MSE) in order to enable performance comparison; this is defined as

$$\text{MSE} \triangleq \mathbb{E} \left[ \left| \frac{\tilde{h}_p - h_p}{h_p} \right|^2 \right]. \quad (14)$$

Note that for an unbiased estimator  $\text{MSE} = \text{Var} \left[ \frac{\tilde{h}_p}{h_p} \right]$ .

a) *Virtual symbol method:* From (9) and (10) for ICM and IAM-R/C, we have

$$y_p = h_p c_p + h_p \sum_{m=p-1}^{p+1} \sum_{n=3}^4 \xi_{m,n}^{p,1} a_{m,n} + w_{p,1} \quad (15)$$

and so

$$\frac{\tilde{h}_p - h_p}{h_p} = \frac{y_p}{h_p c_p} - 1 = \frac{1}{c_p} \left\{ \sum_{m=p-1}^{p+1} \sum_{n=3}^4 \xi_{m,n}^{p,1} a_{m,n} + w_{p,1} \right\}. \quad (16)$$

The  $a_{m,n}$  for  $n \geq 3$  are uncorrelated, real-valued, zero-mean, random data symbols with variance  $\sigma_a^2$ . Taking the expectation with respect to these data symbols we find that  $\mathbb{E} \left[ \frac{\tilde{h}_p - h_p}{h_p} \right] = 0$ , implying that the estimator is unbiased. The normalized variance (or MSE) is given by

$$\text{MSE}_{\text{VS}} = \frac{\sigma_a^2}{|c_p|^2} \left\{ \sum_{m=p-1}^{p+1} \sum_{n=3}^4 |\xi_{m,n}^{p,1}|^2 + \frac{\sigma^2}{\sigma_a^2} \right\}. \quad (17)$$

From this expression, we see that in the limit as  $\sigma^2 \rightarrow 0$  (i.e., in high-SNR conditions), there remains an estimator MSE floor that is inversely proportional to the squared magnitude of the virtual symbol  $c_p$ . Note that, as per Table II (which is computed based on the PHYDYAS filters), this squared magnitude is largest for the IAM-C method, which is why IAM-C has the lowest MSE floor when using the virtual symbol method.

b) *GLS Estimation Method:* Noting that a GLS estimator is unbiased, using (13) we may derive the MSE of the proposed GLS-based estimator as

$$\begin{aligned} \text{MSE}_{\text{GLS}} &= \text{Var} \left[ \frac{\tilde{h}_p}{h_p} \right] = \frac{1}{|h_p|^2} \hat{\mathbf{g}}_p^H \mathbb{E} [\mathbf{y}_p \mathbf{y}_p^H] \hat{\mathbf{g}}_p \\ &= \hat{\mathbf{g}}_p^H \mathbf{\Omega} \hat{\mathbf{g}}_p. \end{aligned} \quad (18)$$

<sup>4</sup>In very highly frequency selective channels, the ‘‘locally constant channel’’ assumption also becomes a limiting factor.

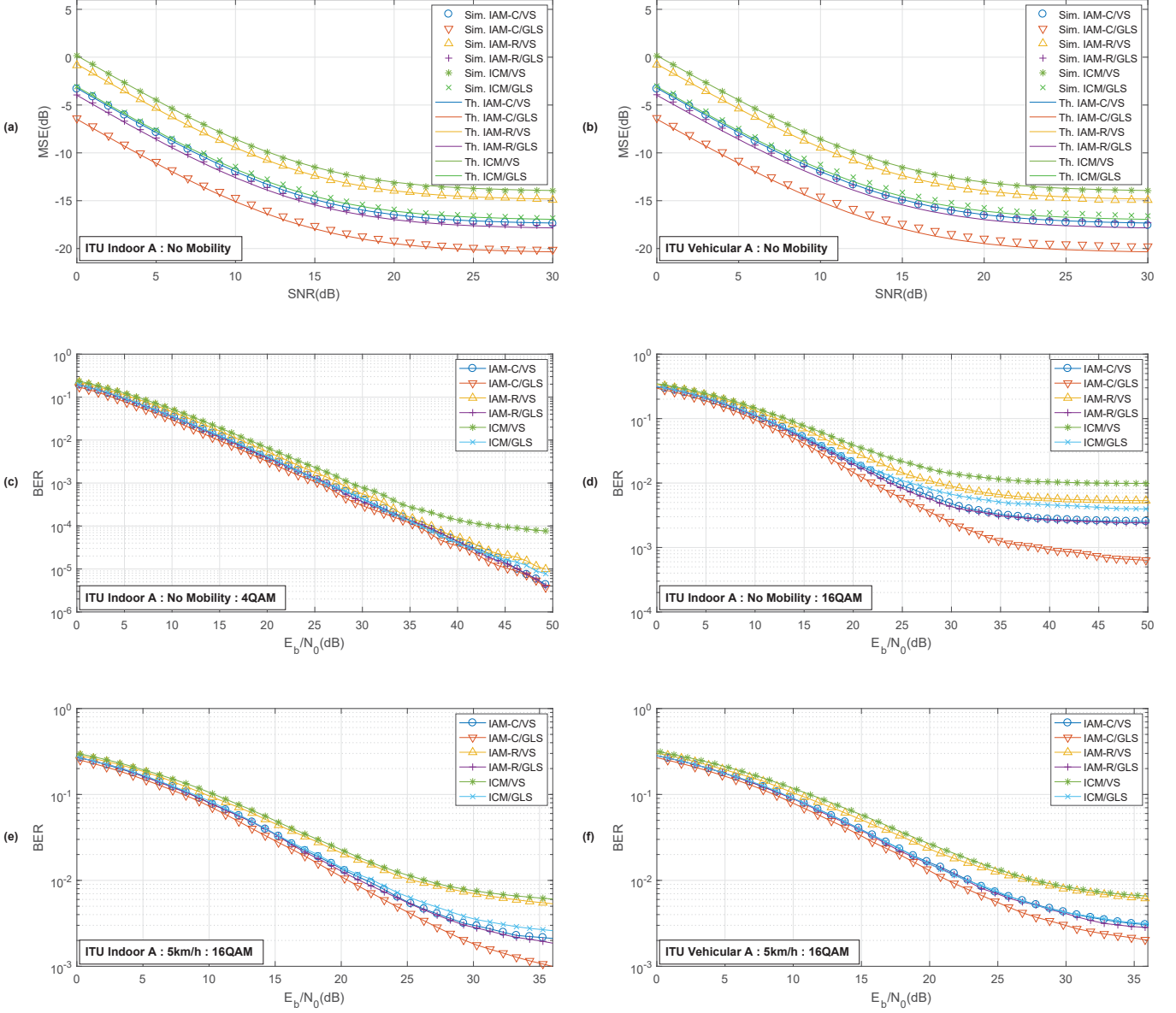


Fig. 2. MSE of different CE techniques using (a) ITU Indoor A channel model and (b) ITU Vehicular A channel model. BER performance curve using no mobility condition for ITU Indoor A channel model with (c) 4-QAM data symbols and (d) 16-QAM data symbols. (e) BER with mobility of 5km/hr with 16-QAM data symbols for ITU Indoor A channel model and (f) BER with mobility of 5km/hr with 16-QAM data symbols for ITU Vehicular A channel model.

Grouping those parts of  $\hat{\mathbf{g}}_p$  that are scalars, we obtain

$$\begin{aligned} \text{MSE}_{\text{GLS}} &= \frac{1}{\left| \mathbf{c}_p^H \hat{\mathbf{\Omega}}^{-1} \mathbf{c}_p \right|^2} \mathbf{c}_p^H \hat{\mathbf{\Omega}}^{-1} \mathbf{\Omega} \left( \mathbf{c}_p^H \hat{\mathbf{\Omega}}^{-1} \right)^H \\ &\approx \frac{1}{\left| \mathbf{c}_p^H \hat{\mathbf{\Omega}}^{-1} \mathbf{c}_p \right|^2} \mathbf{c}_p^H \hat{\mathbf{\Omega}}^{-1} \mathbf{c}_p = \left( \mathbf{c}_p^H \hat{\mathbf{\Omega}}^{-1} \mathbf{c}_p \right)^{-1} \end{aligned} \quad (19)$$

where  $\hat{\mathbf{\Omega}} \triangleq \mathbf{\Omega} \Big|_{\eta=\frac{\sigma^2}{2}}$ , and we have used the approximation  $\hat{\mathbf{\Omega}}^{-1} \mathbf{\Omega} \approx \mathbf{I}$ .

## V. SIMULATION RESULTS AND DISCUSSION

In this section, a simulation study is conducted to compare the performance of different preamble-based channel estimation techniques in terms of CE-MSE and BER, for a low and a medium frequency selective channel model (ITU Indoor A and ITU Vehicular A [11]), along with scenarios of no-mobility and mobility at a velocity of 5km/h. The transmitted signal consists of  $M = 1024$  sub-carriers of 15kHz bandwidth each. The PHYDYAS prototype filter [10] with an overlapping factor of  $K = 4$  is considered. For the case of mobility, the reference frequency is taken to be 2.4 GHz for the calculation of the Doppler spread, with a Jakes Doppler spectrum assumed. Channel tracking over

the FBMC frame for each data symbol is done through linear interpolation of estimates. Each FBMC frame consists of 64 OQAM data symbols, along with 3 preamble OQAM symbols of which the first and third are symbols of nulls and the middle symbol consist of  $\alpha = 1$  (Fig. 1). The OQAM symbols are either derived from 4-QAM or 16-QAM Gray coded symbols normalized such that  $\sigma_a^2 = 1$ . For each SNR or  $E_b/N_0$  value, either a minimum of 3000 frames are transmitted or at least  $10^5$  bit errors are collected. Data symbols are estimated using the estimated channel coefficients through the equalizer in (8).

For the non-time-varying scenario (referred to as “no-mobility” in Fig. 2), CE-MSE for a low (Indoor A) and medium (Vehicular A) frequency selective channel model is shown in Fig. 2(a) and (b) respectively, along with a comparison with the theoretical CE-MSE for each channel estimation scheme. From these results, it can be seen that the proposed GLS-based estimation method outperforms the corresponding VS-based schemes, in each case (i.e., ICM, IAM-R/C) exhibiting almost 3dB better CE-MSE than the VS-based counterpart. In Fig. 2(b), simulation results show a slight deviation from the theoretical values when frequency selectivity is increased (i.e., when we move from ITU Vehicular A to ITU Indoor A) using GLS-based estimation, but it also shows that the assumption of frequency selectivity still holds good even for a medium frequency selective channel. The BER result in Fig. 2(c) shows that the original ICM and IAM-R/C schemes exhibit similar performance to the GLS-based estimation scheme for a wide range of  $E_b/N_0$  when 4QAM modulation is used, but the GLS-based scheme shows a clear BER gain when higher-order QAM (16-QAM) is employed, as is evident in Fig. 2(d), Fig. 2(e) and Fig. 2(f). This is because, while lower-order modulation (i.e., 2-PAM or 4-QAM) are sensitive to phase errors only, higher-order QAM is sensitive to both phase and amplitude errors; thus, the improvement in CE-MSE afforded by GLS-based CE is harnessed by higher-order QAM. From this we may conclude that GLS-based CE scheme is a better option if higher-order QAM is used, consequently making it better for high data rate FBMC-OQAM applications.

Finally, Fig. 2(e) and Fig. 2(f) further verify the robustness of the GLS-based method, which shows a clear BER gain over conventional CE schemes in conditions of mobility. Together these results prove the effectiveness of the GLS-based CE method for FBMC-OQAM transmission, and demonstrate that the GLS-based approach yields a clear CE-MSE and BER advantage for high data rate FBMC-OQAM in various channel/mobility scenarios.

## VI. CONCLUSION

In this paper, the problem of efficient preamble-based channel estimation in FBMC-OQAM systems was revisited, and in particular the problem of alleviating the severe channel estimation error floors in the high-SNR region caused by ICI/ISI suffered by the transmitted symbols. A theoretical analysis of CE-MSE was presented for various conventional VS-based CE schemes such as IAM and ICM, which were shown to agree well with simulation results. We also proposed and analyzed a generalized least squares (GLS) based CE scheme capable of taking into account the correlation of noise and interference among sub-carriers. This scheme was shown to exhibit a CE-MSE improvement of almost 3 dB with respect to the corresponding virtual symbol based approach. Finally, for higher-order modulation schemes, it was shown that such lowering of CE-MSE results in a significant improvement in the system’s bit error rate (BER) performance. This improvement was achieved with only minor complexity increase.

## ACKNOWLEDGMENT

This publication has emanated from research supported by a research grant from Science Foundation Ireland (SFI) and is co-funded under the European Regional Development Fund under Grant Number 13/RC/2077.

## REFERENCES

- [1] P. Banelli, S. Buzzi, G. Colavolpe, A. Modenini, F. Rusek and A. Ugolini, “Modulation Formats and Waveforms for 5G Networks: Who Will Be the Heir of OFDM?: An overview of alternative modulation schemes for improved spectral efficiency”, *IEEE Signal Processing Magazine*, vol. 31, no. 6, pp. 80-93, Nov. 2014.
- [2] E. Kofidis, L.G Baltar, X. Mestre, F. Bader, and V. Savaux. “FBMC Channel Estimation Techniques.” In *Orthogonal Waveforms and Filter Banks for Future Communication Systems*, pp. 257-297. July 2017.
- [3] D. Lacroix, J. P. Javaudin, “A new channel estimation method for OFDM/OQAM”, in *Proceedings of 7th International OFDM Workshop*. Hamburg, Sept. 2002.
- [4] S. W. Kang and K. H. Chang, “A Novel Channel Estimation Scheme for OFDM/OQAM/OTFS System”, *ETRI journal*, 29(4):430-6, Aug 2007.
- [5] D. Katselis, C. R. Rojas, M. Bengtsson and H. Hjalmarsson, “Frequency smoothing gains in preamble-based channel estimation for multicarrier systems”, *Signal Processing*, vol. 93, no. 9, pp. 2777-2782, Jan 2012.
- [6] E. Kofidis and D. Katselis, “Preamble-based channel estimation in MIMO-OFDM/OQAM systems”, in *Proceedings of IEEE International Conference on Signal and Image Processing Applications (ICSIPA)*, Nov. 2011.
- [7] P. Jhonson. “GLS (Generalized Least Squares)”. University of Kansas, USA. [Online]. Available: <http://pj.freefaculty.org/guides/stat/Regression/GLS/GLS-1-guide.pdf>
- [8] S. M. Key, “Fundamentals of statistical signal processing: estimation theory, Englewood Cliffs, NJ: Prentice-Hall Int., 1993.
- [9] A. Viholainen, M. Bellanger, M. Huchard “PHYDYAS project, deliverable 5.1: Prototype filter and structure optimization. FP7-ICT”, Tech. Rep., Jan. 2010.
- [10] M. Bellanger, “Specification and design of a prototype filter for filter bank based multicarrier transmission”, in *Proceedings of IEEE International Conference on Acoustics, Speech, and Signal Processing (ICASSP)* vol. 4, Salt Lake City, UT, pp. 2417-2420, May 2001.
- [11] R. Jain, “Channel models: A tutorial”, in *Proceedings of WiMAX Forum AATG*, pp. 121, Feb. 2007.